



Advancements in Modified-release Oral Drug Delivery: Delivery Throughout the Gastro-intestinal tract

# Development of a Novel Bilosomal System for Improved Oral Bioavailability of Sertraline Hydrochloride: Formulation Design, In Vitro Characterization, and Ex Vivo and In Vivo Studies

Aliaa Ismail<sup>1</sup> · Mohammed Teiama<sup>1</sup> · Basma Magdy<sup>1</sup> · Wedad Sakran<sup>1</sup>

Received: 21 February 2022 / Accepted: 20 June 2022 / Published online: 8 July 2022  
© The Author(s) 2022

## Abstract

This study was proposed to develop an optimized sertraline hydrochloride (SER)-loaded bilosomal system and evaluate its potential for enhancement of drug oral bioavailability. A full  $2^3$  factorial design was used to prepare SER-loaded bilosomal dispersions by thin film hydration using span 60, cholesterol (CHL), and sodium deoxycholate (SDC). The investigated factors included the total concentration of span 60 and CHL ( $X_1$ ), span 60:CHL molar ratio ( $X_2$ ), and SER:SDC molar ratio ( $X_3$ ). The studied responses were entrapment efficiency ( $EE\%$ ) ( $Y_1$ ), zeta potential ( $Y_2$ ), particle size ( $Y_3$ ), and in vitro % drug released at 2 ( $Y_4$ ), 8 ( $Y_5$ ), and 24 h ( $Y_6$ ). The selected optimal bilosomal dispersion (N1) composition was 0.5% w/v ( $X_1$ ), 1:1 ( $X_2$ ), and 1:2 ( $X_3$ ). Then, N1 was freeze dried into FDN1 that compared with pure SER for in vitro drug release, ex vivo permeation through rabbit intestine, and in vivo absorption in rats. Moreover, storage effect on FDN1 over 3 months was assessed. The optimal dispersion (N1) showed  $68 \pm 0.7\%$  entrapment efficiency,  $-41 \pm 0.78$  mV zeta potential, and  $377 \pm 19$  nm particle size. The freeze-dried form (FDN1) showed less % drug released in simulated gastric fluids with remarkable sustained SER release up to 24 h compared to pure SER. Moreover, FDN1 showed good stability, fivefold enhancement in SER permeation through rabbit intestine, and 222% bioavailability enhancement in rats' in vivo absorption study compared to pure SER. The SER-loaded bilosomal system (FDN1) could improve SER oral bioavailability with minimization of gastrointestinal side effects.

**Keywords** Nano-vesicular carriers · Factorial design · Bile salts · Entrapment efficiency · Thin film hydration

## Introduction

Sertraline hydrochloride (SER) is an anti-depressant drug that belongs to selective serotonin reuptake inhibitors (SSRIs) class. It is widely prescribed for the treatment of major depressive disorders and other mental health disorders including obsessive-compulsive disorder (OCD), panic disorder, post-traumatic stress disorder, premenstrual dysphoric disorder, and social phobia in a dose range of 25–200 mg/day orally [1, 2]. SER is a hydrochloride salt of a weak base (pKa 9.48) that belongs to the biopharmaceutical

classification system (BCS) class II drugs which are characterized by poor aqueous solubility that critically limits its dissolution rate. The salt shows pH-dependent solubility with highest solubility at pH 4.5, and it turns back into its original base form when it enters the intestinal region making aggregates which suppress its absorption [3, 4]. Additionally, SER undergoes extensive first-pass metabolism in the liver. As a result of low solubility, poor absorption, and extensive first-pass hepatic metabolism, SER shows low oral bioavailability (~44%). Thus, there is a great demand for strategies to improve SER bioavailability [2, 4]. Moreover, it was reported that direct contact of SER with the upper gastrointestinal tract (GIT) results in many side effects including nausea, vomiting, and regurgitation especially with high doses. Therefore, minimizing gastric exposure by sustaining the release of SER is desirable to reduce these dose-related side effects [5].

✉ Aliaa Ismail  
aliaa\_adly@pharm.helwan.edu.eg

<sup>1</sup> Department of Pharmaceutics and Industrial Pharmacy, Faculty of Pharmacy, Helwan University, Ain Helwan, Cairo 11795, Egypt

Several reported approaches were adapted for improving SER oral bioavailability including enterically coated sustained release matrix tablet [5], complexation with cyclodextrin and incorporation into orodispersible tablet [2], crystal modification [4], solid lipid nano-particles [6], and self-nano-emulsifying drug delivery system (SNEDDS) [3].

In recent studies, many colloidal vesicular carriers including liposomes, niosomes, and bilosomes have shown obvious advantages over conventional dosage forms in oral drug delivery [7]. They can improve solubility and dissolution rates of the drug as well as enhance drug lymphatic transport and thus bypassing the first-pass metabolism leading to improved oral bioavailability [8, 9]. Unfortunately, conventional liposomes and niosomes are subjected to chemical and enzymatic destabilization in the GIT which limits their application in the oral drug delivery [7, 10]. However, incorporating bile salts within these vesicles makes them more resistant to harsh GIT environment destabilization than conventional vesicles and able to protect the entrapped drug to a higher extent after oral delivery [11]. Bilosomes are elastic nano-sized colloidal carriers similar to niosomes in structural composition (non-ionic surfactant and cholesterol) but incorporating bile salts. Bile salt acts also as permeability enhancer through biological barriers including the intestinal membrane and blood brain barrier (BBB). Moreover, Bile salt gives the vesicles a negative charge which provide higher storage stability and promote drug uptake through M-cells in the Peyer's patch followed by cellular processes which extend into the underlying lymphoid tissue leading to drug transport via intestinal lymphatic system as well as the avoidance of hepatic first pass metabolism [7, 11]. Bilosomes have been reported to enhance oral bioavailability of many drugs as reported in several literatures [7, 12–14].

The aim of this study was to develop SER-loaded bilosomal system as a new oral carrier for SER. A full  $2^3$  factorial design was used to statistically analyze the effect of formulation variables followed by selection of the optimal bilosomal formula by numerical optimization. Freeze drying was then conducted on the optimized formula to prepare a SER-loaded bilosomal powder. The freeze-dried form of the optimal formula was further evaluated for ex vivo intestinal permeation and in vivo absorption study in comparison with pure SER powder.

## Materials and Methods

### Materials

Sertraline hydrochloride (SER) was kindly donated as a gift by Pharco Pharmaceuticals (Alexandria, Egypt). Sorbitan mono-stearate (span 60) was purchased from Oxford

Laboratory (Mumbai, India); cholesterol (CHL) and sodium deoxycholate (SDC) were purchased from Alpha Chemika (Mumbai, India). Loperamide hydrochloride (internal standard) was purchased from Sigma-Aldrich (St. Louis, MO). HPLC grade methanol, chloroform, acetonitrile, formic acid, and ethyl acetate were purchased from Sigma-Aldrich (Steinheim, Germany). Disodium hydrogen phosphate and monosodium di-hydrogen phosphate were purchased from El Nasr Pharmaceutical Chemicals Company (Abu Zaabal, Egypt); sodium lauryl sulfate (SLS) and hydrochloric acid 30% were purchased from Al-Gomhoria Company for medicines and medical supplies (Cairo, Egypt). All other chemicals were of analytical grade.

### Methods

#### DSC

The compatibility of SER with bilosomal ingredients was investigated by DSC. The DSC thermograms of pure SER, span 60, CHL, and SDC, the 1:1 (w/w) binary physical mixtures of SER with each ingredient, and the quaternary physical mixture of SER with all ingredients in equal weight ratio (1:1:1:1) were recorded using a differential scanning calorimeter (DSC-50, Shimadzu; Kyoto, Japan). Samples (4 mg) were weighed accurately, placed in standard aluminum pan, and heated at a constant heating rate of 10°C/min from 25°C to a temperature of 400°C under a flow of nitrogen gas with flow rate 25 ml/min to avoid sample oxidation [15, 16].

#### FTIR

The compatibility of SER with bilosomal ingredients was further investigated using FTIR. The FTIR spectra of pure SER, span 60, CHL, and SDC and the physical mixtures of SER with other bilosomal ingredients described previously in the “DSC” section were recorded using IR Spectrophotometer (Shimadzu 8400S, Lab Wrench, Japan). The samples were finely grinded with 100 mg of dry potassium bromide powder, compressed into transparent disc, and scanned over the range 400 to 4000/cm [16].

#### Experimental Design

A full  $2^3$  factorial design was constructed to study the effect of formulation variables on the preparation of SER-loaded bilosomal dispersions using Design-Expert® version 13.0.5.0 software (Stat-Ease, Inc., Minneapolis, MN, USA). As presented in Table I, the study design involved three formulation factors (independent variables) at two different levels and these studied factors were assessed for their effects on six selected responses (dependent variables).

ANOVA was generated for responses experimental data. The selection of best fit model for each response, either main effect (one-factor effect), 2-factor interaction (2FI), or 3-factor interaction (3FI) based on estimation of the statistical parameters, predicted  $R^2$  and predicted residual error sum of squares (PRESS). Thereafter, ANOVA statistical analysis for the best-fitted factorial model was approved to evaluate the level of significance of effect of the tested factors as well as their interactions on the responses. A statistically significant level was considered at  $P < 0.05$ .

**Preparation of SER-Loaded Bilosomal Dispersions**

Eight SER-loaded bilosomal dispersions (N1–N8) were prepared by thin film hydration method using a mixture of surfactant (span 60) and CHL with incorporation of a bile salt (SDC) [17, 18]. SER-loaded bilosomal formulae were prepared by dissolving 50 mg of SER and the calculated amounts of span 60 and CHL in 21 ml chloroform: methanol mixture (2:1 v/v) in 250-ml rounded bottom flask. Then, the solution was evaporated in a rotary evaporator (IKA, HBIO basic, RV10B S99, Deutschland, Germany) under reduced pressure at 60°C and 120 rpm for 30 min, till formation of a dried thin film on the inner wall of the flask. Thereafter, the dried thin layer was hydrated with 30 ml of distilled water pre-warmed at 58–60°C containing the desired amount of SDC under normal pressure at temperature just above the glass transition temperature ( $T_g$ ) of span 60 (58°C). The hydration process was done at 120 rpm for 1 h in the presence of small glass beads 5 mm in diameter to confirm complete hydration and formation of SER-loaded bilosomes. The developed dispersion systems were probe sonicated for 3 min at room temperature to achieve particle size uniformity. Moreover, blank bilosomal dispersions were prepared with the same procedure in the absence of SER and stored with the SER-bilosomal dispersions at 4°C till further investigation.

**Characterization of SER-Loaded Bilosomal Dispersions**

**EE%** The percentage of SER entrapped in each formula was measured in triplicate using direct method. One milliliter of each formula and its corresponding blank was centrifuged using a cooling centrifuge at 4°C and 20,000 rpm for 1 h. The supernatant was discarded, and the bilosomal pellets were washed and re-suspended in distilled water to ensure the complete removal of the un-entrapped SER. The obtained dispersion was re-centrifuged, and the collected pellets were dissolved and vortexed with 3 ml of pure chloroform for 1 min in order to disassemble the bilosomal particles and, then, further dilution of dispersion with 10 ml methanol to dissolve all the entrapped SER. The same technique was applied on the blank bilosomal pellets, and the concentration of SER in the obtained methanol solution of each SER-loaded pellets was determined by measuring its UV absorbance against the methanolic solution of its corresponding blank pellets at 274 nm using a UV/visible spectroscopy (Jasco spectrophotometer, Japan) [19]. The entrapment efficiency ( $EE\%$ ) of SER was calculated according to the following equation:

$$EE\% = \frac{\text{Amount of entrapped SER}}{\text{Original amount of SER added}} \times 100 \quad (1)$$

**Zeta Potential and Particle Size** The zeta potential, vesicular size, and polydispersity index ( $PDI$ ) of all bilosomal dispersions were determined using dynamic light scattering integrated in Malvern Zetasizer (Malvern instruments/Worcestershire, UK). Bilosomal samples were 100-fold diluted with de-ionized water and measured in triplicate at  $25 \pm 0.5^\circ\text{C}$ .

**In Vitro Drug Release from SER Bilosomal Dispersions**

The bilosomal pellets equivalent to 15 mg SER (separated by cooling centrifugation at 4°C and 20,000 rpm for 1 h

**Table 1** Various independent and dependent variables used in the factorial design for preparation of SER-loaded bilosomal dispersions

Independent variables (Factors)	Levels	
	Low (-1)	High (+1)
$X_1$ = total concentration of span 60 and CHL (%w/v)	0.5	1
$X_2$ = span 60:CHL molar ratio	1	7
$X_3$ = SER:SDC molar ratio	0.25	0.5
Dependent variables (responses)	Constraints (goals)	
$Y_1$ = entrapment efficiency (%)	Maximize	
$Y_2$ = zeta potential (mV)	Maximize	
$Y_3$ = particle size (nm)	Minimize	
$Y_4$ = cumulative drug released at 2 h (%)	Minimize	
$Y_5$ = cumulative drug released at 8 h (%)	Maximize	
$Y_6$ = cumulative drug released at 24 h (%)	Maximize	

CHL cholesterol, SDC sodium deoxycholate, SER sertraline hydrochloride

and washed with distilled water) of the different bilosomal formulations were re-suspended and vortexed with 7 ml of distilled water. The *in vitro* release of SER from the obtained bilosomal dispersions was performed using dialysis method described by Jadon et al., Khan et al., and Song et al. [20–22] with slight modifications.

Before testing, dialysis tubing cellulose membrane (molecular weight cutoff 12,000–14,000 Da, Sigma-Aldrich, St. Louis, MO) pieces of 7 cm length and 3.5 cm width were soaked overnight in de-ionized water. The drug release study was performed for 24 h using two consecutive release media, 0.1 N HCl (pH 1.2) as a simulated gastric fluid (SGF) for the initial 2 h, and 0.1 M phosphate buffer (pH 6.8) containing 1% SLS as a simulated intestinal fluid (SIF) for the remaining 22 h. The bilosomal dispersion was filled in the dialysis bag and tightly closed from the two ends using rubber bands. The dialysis bag was then immersed in 80 ml of 0.1N HCl (pH 1.2) for 2 h, then removed, and washed with distilled water. Thereafter, the dialysis bag was re-immersed for further 22 h in 20 ml of 0.1 M phosphate buffer (pH 6.8) containing 1% SLS. The release medium was stirred magnetically at 100 rpm, and the temperature was maintained at  $37 \pm 0.5^\circ\text{C}$  using digital hot plate stirrer (Witeg laboratory GmbH, Wertheim, Germany). At various time intervals 0.5, 1, 2, 3, 4, 6, 8, and 24 h of the release study, 3-ml samples were withdrawn and immediately replaced with 3 ml of fresh medium to keep constant volume and sink conditions. The samples were filtered with sterile syringe filter (0.22  $\mu\text{m}$ ) and analyzed spectrophotometrically at 273 nm and 275 nm for 0.1 N HCl and 0.1 M phosphate buffer containing (1% SLS), respectively. The release studies were carried out in triplicate, and then, mean values were plotted as percentage cumulative drug release against time.

### Release Kinetics and Mechanisms

The *in vitro* release data obtained were fitted to various kinetic models such as zero order (cumulative % drug released versus time), first order (log cumulative % drug remained versus time), and Higuchi's model (cumulative % drug released versus square root of time). The correlation coefficient ( $R^2$ ) was determined for each model, and the best fitting model was selected depending on the highest correlation coefficient ( $R^2$ ) value [23].

Moreover, release data were further analyzed according to Korsmeyer and Peppas model [24] given by the following equation:

$$M_t/M^\infty = Kt^n \quad (2)$$

where  $M_t$  is the amount of drug released at time  $t$ ,  $M^\infty$  is the amount of drug released at infinite time,  $K$  is the kinetic constant, and  $n$  is the release exponent indicative

of the release mechanism. The  $n$  values used for explication of drug release mechanism from the prepared bilosomal dispersions were determined from the slope of the plot of log cumulative percent of drug release ( $\leq 60\%$ ) versus log time, where  $n \leq 0.45$  indicates a Fickian diffusion mechanism. Values of  $0.45 < n < 0.89$  corresponds to non-Fickian anomalous transport while  $n = 0.89$  corresponds to case II (polymer relaxational transport). If  $n > 0.89$ , this indicates super case II transport.

### Optimization of SER-Loaded Bilosomal Dispersions

In order to determine the optimal formula for further investigations, a numerical optimization technique by the desirability approach was performed utilizing Design-Expert® software according to the constraints (goals) listed in Table I. The  $X_1$ ,  $X_2$ , and  $X_3$  were kept within the range used in the present study. On the basis of these assigned goals, software determines the possible formulation composition with maximum desirability value.

### TEM

The morphology of the optimal SER-loaded bilosomal dispersion (N1) was examined using transmission electron microscopy (TEM). The freshly prepared bilosomal system was diluted with deionized water, and one drop was placed on a carbon coated copper mesh and left to dry to allow the adhesion of bilosomes to the carbon substrate. Then, it was stained with 1% w/v phosphotungstic acid dye and the mesh was subjected to air drying for 10 min at room temperature. The stained sample was then visualized using TEM (JEOLJEM-1400, USA) and photographs were taken at adequate magnifications.

### Preparation of SER-Loaded Bilosomal Powder

The bilosomal powder of the optimal formula (N1) was prepared using the freeze-drying technique as described by Ferreira et al. and Marín et al. [25, 26] with slight modifications. In 50-ml falcon tubes, the freshly prepared bilosomal dispersions of N1 were centrifuged using a cooling centrifuge at  $4^\circ\text{C}$  and 20,000 rpm for 1 h. The supernatants were discarded, and the obtained bilosomal pellets in each falcon tube were washed carefully for three times with distilled water and re-centrifuged at  $4^\circ\text{C}$  and 20,000 rpm for 1 h to ensure the complete removal of the un-entrapped SER. Then, the washed bilosomal pellets were vortexed and re-suspended with 10 ml of distilled water. The produced dispersions were poured into plastic cups with perforated caps and initially frozen at  $-20^\circ\text{C}$  for 24 h. Then, the lyophilization

process was carried out using a freeze dryer (Christ Alpha 1–2 LD; Osterode am Harz, Germany) coupled to a vacuum pump (Vacubrand GmbH + Co. KG; Wertheim, Germany) operating at a vacuum level of 0.035 mbar, at a temperature of  $-58$  to  $-60^{\circ}\text{C}$ . The same procedure was applied on a blank formulations have the same composition of N1 except for the drug. The obtained freeze-dried SER-loaded bilosomal powder (FDN1) and the freeze-dried blank powder were stored in a desiccator at  $25^{\circ}\text{C}$  for further studies.

### Determination of Drug Loading (%) in Freeze-Dried Bilosomal Powder

Ten mg of the FDN1 powder were weighed accurately and dissolved in a mixture of 10 ml methanol and 3 ml chloroform. The concentration of SER in the obtained solution of the FDN1 powder was determined by measuring its UV absorbance at 274 nm against the solution of the blank bilosomal powder (the same FDN1 formula composition in the absence of drug). The % drug loading was calculated using the following formula [27]:

$$\text{Drug loading (\%)} = \frac{\text{Weight of SER in the bilosomal powder}}{\text{Weight of the bilosomal powder}} \times 100 \quad (3)$$

Furthermore, the % drug loading and *EE*% were compared before and after lyophilization of the optimized bilosomal formula.

### In Vitro Release from the Freeze-Dried Bilosomal Powder

The release of SER from FDN1 powder was compared with its release from pure SER. The release experiment was conducted by the dialysis bag technique using USP II dissolution apparatus (Hanson Research, CA, USA) [22, 28]. Amounts of either FDN1 or pure SER equivalent to 25 mg SER were sealed into the dialysis bags with two ends closed tightly using rubber bands. Thereafter, each dialysis bag was tied to a paddle and immersed in 200 ml of 0.1 N HCl (pH 1.2) for 2 h as a SGF release medium. Then, dialysis bags were removed from 0.1 N HCl, washed with distilled water, and re-immersed in 50 ml of 0.1 M phosphate buffer (pH 6.8) containing 1% SLS till the end of experiment. The stirring speed and temperature were maintained at 100 rpm and  $37^{\circ}\text{C} \pm 0.5^{\circ}\text{C}$ , respectively. At various time intervals (1, 2, 3, 4, 6, 8, 10, 12, 16, 20, and 24 h) of the release study, 3-ml samples were withdrawn out from the release medium and immediately compensated with 3 ml of fresh medium to keep up constant volume and sink conditions. The samples were filtered with sterile syringe filter 0.22  $\mu\text{m}$ , and the amount of SER released was determined spectrophotometrically at

273 nm and 275 nm for 0.1 N HCl and 0.1 M phosphate buffer containing (1% SLS), respectively. The experiment was performed in triplicate, and the cumulative release percent of SER was calculated.

The in vitro release mechanism of SER from FDN1 was determined by fitting the release data with different mathematical models; zero order kinetics, first order kinetics and Higuchi diffusion models. Also, Korsmeyer and Peppas model was applied and the exponent (*n*) value was calculated as it lights up other mechanisms of drug release [23].

### Studies of Storage Effect on Bilosomal Powder (FDN1)

Samples of the prepared bilosomal powder (FDN1) were stored for 3 months at  $25^{\circ}\text{C}$  in a desiccator. The stability of FDN1 upon storage was assessed in terms of zeta potential, particle size, *PDI*, and % drug loading. The samples were analyzed after 0, 1, and 3 months for the previously mentioned characters. Moreover, the in vitro drug release was performed on the FDN1 powder after 0, 1, and 3 months of storage. Then, dissolution efficiency % (*DE*%) values after 2, 8, and 24 h of release profiles after 0, 1, and 3 months storage were calculated according to the following equation [29]:

$$DE\% = \frac{\int_0^t y \times dt}{y_{100} \times t} \times 100 \quad (4)$$

where (*DE*%) is as the area under the dissolution curve up to a definite time (*t*) expressed as a percentage of the area of the rectangle described by 100% dissolution in the same time. The term (*y*) symbolizes the drug percent dissolved at time (*t*). Areas under the curves were calculated using the trapezoidal method.

The data acquired after 1 and 3 months for all the assessed stability terms were analyzed for statistical significance with data at zero time by Student's *t* test using Microsoft Office 2007, Excel package. A statistically significant difference was considered at ( $P < 0.05$ ). All measurements for storage effect studies were performed in triplicate ( $n = 3$ ).

### HPLC Assay of SER

The HPLC analysis was performed according to a reported method [30] with slight modifications. The HPLC system consisted of HPLC Agilent 1200 LC-Quaternary series pump (Agilent technologies Inc., Santa Clara, CA, USA) coupled to Waters UV/visible detector (Waters Corporation, Milford, MA, USA). The used column was XBridge™ C18 column (5  $\mu\text{m}$ ,  $4.6 \times 250$  mm, Waters Corporation, Milford, MA, USA), and the column temperature was maintained

at 35°C. A mobile phase consisting of 10 mM ammonium formate buffer (pH 4.5) and acetonitrile was used at 20:80 (v/v) ratio in an isocratic elution mode at a flow rate of 1.3 ml/min. The detector wavelength was fixed at 220 nm, and samples were injected at injection volume of 20 µl using a manual injector.

### Validation of the HPLC Assay

The assay method was validated in terms of linearity, accuracy, and precision (intra-day and inter-day). The accuracy and precision determination were carried out with three replicates of three different concentrations of 25 µg/ml (low-quality control, LQC), 75 µg/ml (medium-quality control, MQC), and 175 µg/ml (high-quality control, HQC) samples.

### Ex Vivo Drug Permeation Study

Ex vivo permeation for SER-loaded bilosomal powder (FDN1) was compared to pure SER using fresh rabbit gut. The protocol of this study was authorized by the Animal Ethics Committee of Faculty of Pharmacy, Helwan University, No. 03A2021. The aspects of animal handling in this study were conformed to the EU directive 2010/63/EU guidelines for animal experiments. One male rabbit weighing 2.5 kg was fasted overnight before starting the experiment. The anaesthetized rabbit was sacrificed, and the small intestine was separated and cut off into small pieces of 7 cm length and 0.5 cm diameter. The calculated surface area for each obtained intestinal sac membrane was approximately 11 cm<sup>2</sup>.

The intestinal sacs were flushed with warm saline solution to remove food residues and to be ready for the ex vivo permeability experiment. The pure SER suspension (5 ml) and the FDN1 powder suspension (5 ml) equivalent to 25 mg SER were filled into the mucosal side of the intestinal sac using a syringe, and both ends of the sac were ligated tightly with a thread [31]. Then, each intestinal sac was tied with a paddle rotating at 50 rpm in 70 ml of phosphate buffer (pH 7.4) containing 1% SLS kept at 37 °C. The experimented was carried out for 8 h in USP II dissolution apparatus (Hanson Research, CA, USA) under continuous aeration using aerator [32]. One-milliliter samples were withdrawn from the permeation medium at predetermined time intervals (1, 2, 3, 4, 6, and 8 h) and replenished with the same volume of a fresh one to maintain the sink conditions. The study was carried out in triplicate, and the collected samples were filtered using a sterile syringe filter (0.22 µm), and the amount of SER permeated through the sac was determined using HPLC method. Then, a graph between the cumulative amounts of SER permeated per unit area of rabbit intestine (µg/cm<sup>2</sup>) versus time (h) was plotted. The slope of the graph

was taken as permeation flux to calculate the apparent permeability coefficient (APC) as follows [12, 33, 34]:

$$APC_{(cm/h)} = \frac{\text{Flux}_{(\mu\text{g}/\text{cm}^2/\text{h})}}{C_{0(\mu\text{g}/\text{ml})}} \quad (5)$$

where  $C_0$  represents the initial concentration of SER in the mucosal side (donor compartment).

The enhancement ratio (ER) of the FDN1 powder was then calculated using the following Eq. (13):

$$\text{Enhancement ratio (ER)} = \frac{APC \text{ of the bilosomal FDN1 powder}}{APC \text{ of the drug}} \quad (6)$$

### In Vivo Absorption Study

**Experimental Animals** Ten adult healthy female Wistar rats with average body weight of  $250 \pm 17$  g were enrolled in the study. The rats were randomly divided into two groups of equal size (5 rats each), and each group was housed in a separate cage and supplied with food and water. The protocol of the study was authorized by the Animal Ethics Committee of Faculty of Pharmacy, Helwan University, No. 03A2021. The use and treatment of animals enrolled in this study complied with the EU directive 2010/63/EU for animal experiments.

**Dose Calculation for Rat** The human daily dose of SER was reported to be ranged from 0.7 to 2.9 mg/kg [35]. The rat equivalent dose was calculated by multiplication of the average SER human daily dose (1.8 mg/kg) by the  $K_m$  ratio [36].

$$K_m \text{ ratio} = K_m \text{ Human} / K_m \text{ Rat} \quad (7)$$

where  $K_m$  symbolizes a correction factor estimated by dividing the average body weight (kg) of species to its body surface area (m<sup>2</sup>).

The value of  $K_m$  ratio for converting human dose into rat equivalent dose was 6.2 (36). Thus, the calculated rat equivalent dose was found to be 11.16 mg SER/kg.

### Study Design

In vivo drug absorption study was performed to evaluate the rate and extent of oral absorption of SER from the optimized freeze-dried SER-loaded bilosomal powder (FDN1) compared to pure SER. In this study, rats were fasted overnight before drug administration and continued fasting until 2 h post dose, with water allowed. Rats were divided randomly into two groups (A) and (B). Each rat in group (A) received a single oral dose of the prepared formula (FDN1) powder equivalent to (11.16 mg SER/kg), while rats in group

(B) received single oral dose of the pure drug equivalent to (11.16 mg SER/kg). The formula FDN1 and pure SER were administered orally to the rats along with 4 ml of water (in form of aqueous suspension) using a feeding tube. One-milliliter orbital sinus blood samples were collected directly from each rat under anesthesia into heparinized tubes using heparinized capillary needle at 0 (pre-dose), 0.25, 0.5, 1, 2, 4, 6, 8, 12, and 24 h post dose. Plasma was separated immediately from the blood cells by centrifugation at 4000 rpm for 10 min and stored frozen at  $-80^{\circ}\text{C}$  until analysis.

### Analysis of SER Plasma Levels

The SER plasma levels were determined using liquid chromatography–tandem mass spectrometry (LC–MS/MS) adapted from a reported method with some modifications [37, 38]. One hundred microliters of the internal standard (loperamide hydrochloride) stock solution (100 ng/ml) was added to 0.5 ml of each plasma sample and vortexed for 1 min. Then, SER extraction solvent (4 ml ethyl acetate) was added and the samples were vortexed for 5 min on a rocker-mixer Reax II (Heidolph, Schwabach, Germany). Thereafter, samples were centrifuged for 10 min at 4000 rpm and  $4^{\circ}\text{C}$  using (Eppendorf centrifuges 5804 R). The upper organic layer was separated and transferred into new Wassermann tubes and evaporated to dryness using vacuum concentrator (Eppendorf 5301; Hamburg, Germany). The dried residues were reconstituted with 500  $\mu\text{l}$  of the mobile phase (acetonitrile:0.1% formic acid in water (80:20, v/v)). Then, tubes were vortexed for 1 min and finally transferred to the auto sampler vials where 10  $\mu\text{l}$  was injected into the LC–MS/MS and analyzed. Additional LC–MS/MS analysis details are described in Online Recourse 1.

### Statistical Analysis of Pharmacokinetic Parameters

The pharmacokinetic parameters following oral administration of the treatments were estimated for each rat in each group. The maximum SER plasma concentration ( $Cp_{\text{max}}$ , ng/ml), the time to reach  $Cp_{\text{max}}$  ( $T_{\text{max}}$ , h), and the area under the plasma concentration–time curve from time zero to 24 h ( $AUC_{0-24}$ , ng h/ml) were obtained from the individual plasma concentration–time curves. The values of the  $Cp_{\text{max}}$  and  $T_{\text{max}}$  were obtained directly from plasma data while the  $AUC_{0-24}$  was calculated using the trapezoidal rule method. The relative bioavailability % ( $Fr$  %) of SER-loaded bilosomal powder (FDN1) was calculated in comparison to the Pure SER as follows:

$$Fr = \frac{AUC_{0-24}(\text{FDN1}) \times \text{Dose}(\text{PureSER})}{AUC_{0-24}(\text{PureSER}) \times \text{Dose}(\text{FDN1})} \times 100 \quad (8)$$

The obtained pharmacokinetic parameters ( $Cp_{\text{max}}$  and  $AUC_{0-24}$ ) were analyzed by Student's  $t$  test using Microsoft Office 2007, Excel package, while  $T_{\text{max}}$  values were analyzed by the non-parametric Mann–Whitney test using GraphPad Instat® (version 3.05). A  $P$ -value  $< 0.05$  was considered statistically significant difference.

## Results and Discussion

### DSC

DSC was performed to reveal the drug characteristics like polymorphic state, stability, and purity and to detect possible interactions between SER and excipients of bilosomal system [39]. As shown in Fig. 1, pure SER exhibited four endothermic peaks at 211, 221, 250.5, and  $287.61^{\circ}\text{C}$  which assured the crystalline nature of SER and indicated its presence in the thermodynamically most stable polymorph (form I) [40]. The first endothermic peak observed at  $211^{\circ}\text{C}$  represented the solid–solid transition of form I to form III. The endothermic peak at  $221^{\circ}\text{C}$  was corresponding to the melting point of traces of form I that bypassed the solid–solid transition of form I to form III. The sharp endothermic peak appeared at  $250.5^{\circ}\text{C}$  was due to the melting point of the in situ generated form III, immediately followed by a comparatively larger endotherm at  $287.61^{\circ}\text{C}$  corresponding to the rapid thermal decomposition and degradation of SER [4, 40]. Regarding SDC, its thermogram revealed the presence of a broad endothermic peak at  $114^{\circ}\text{C}$  possibly due to the loss of water molecules, with subsequent re-crystallization exothermic peak at  $197.33^{\circ}\text{C}$  followed by sharp endothermic peak at  $351.63^{\circ}\text{C}$  corresponding to SDC melting point [41, 42]. Span 60 had a narrow and sharp characteristic endothermic peak at  $56.95^{\circ}\text{C}$  corresponding to its glass transition temperature ( $T_g$ ) [19], whereas CHL showed a broad endothermic melting transition started at  $40^{\circ}\text{C}$  due to the loss of water molecules and a sharp endothermic melting peak at  $145.45^{\circ}\text{C}$  followed by rapid degradation of CHL [16, 41]. The distinctive melting points ( $T_m$ ) of SER, SDC, span 60, and cholesterol were displayed in the DSC thermograms of all physical mixture samples proving SER–excipients compatibility and the absence of interactions, whereas any difference found in the peak intensity, shape or height-to-width ratio, and slight peak temperature shifting may be due to the dilution effect of SER with the excipients [2, 43].

### FTIR

The possible interactions between SER and the investigated excipients were also evaluated using FTIR (Fig. 2).

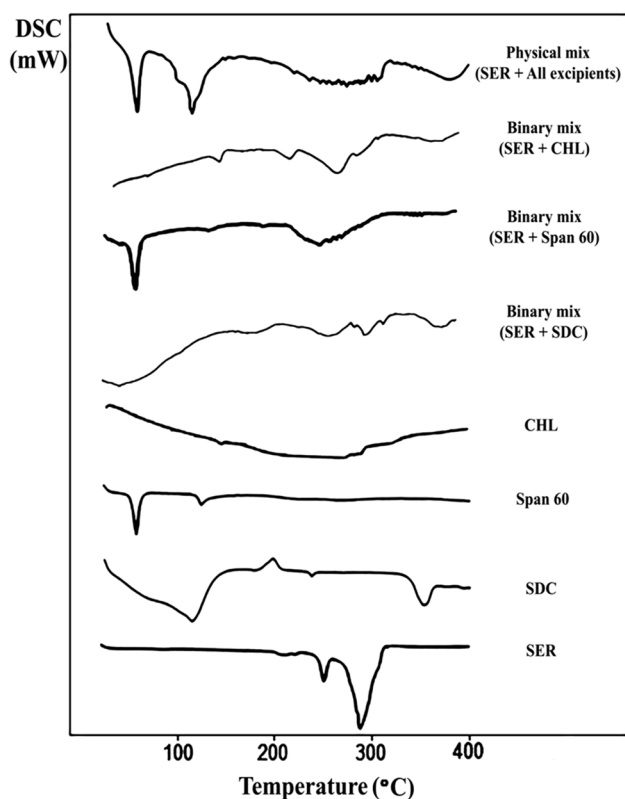


**Fig. 1** DSC thermograms of SER and different bilosomal forming excipients

As shown in Fig. 2A, the IR spectrum of SER was characterized by the following absorption peaks: C–H stretching of N-bonded  $\text{CH}_2$  group at 2939.5/cm; vibrational peaks of aliphatic amine N–H at 2468.88 and 1138/cm; aromatic ring stretching of C–C and C–H at 1581.63 and 1562.34/cm, respectively;  $\text{CH}_3/\text{CH}_2$  scissoring vibrations at 1469.76/cm; C–C ring vibrations at 1651.07/cm; symmetrical and asymmetrical vibrational peaks were observed between 1429 and 1404/cm which attributed to  $\text{CH}_2/\text{NH}_2$  group symmetric deformation and C–H deformation of  $\text{CH}_3/\text{NH}$  group, respectively; vibrational peaks of C–N at 1211.30/cm; the harmonic C–H deformation of aromatic ring vibrational peaks was found between 1056 and 921.97/cm; out-of-plane deformation modes of C–H of the aromatic rings and C–Cl were observed around 825.53/cm; and finally, vibrational peaks of C–Cl at 786.96 and 744.52/cm [2, 5, 39, 44]. The IR spectrum of SDC (Fig. 2B) showed a significant broad absorption peak appeared at 3390.86/cm which attributed to hydroxyl group stretching. Moreover, characteristic vibrational peak were found at 2938.10 and 2862.36/cm for C–H, 1558.48 for  $\text{COO}^-$ , and 1064/cm for C–O [45]. Span 60 spectrum (Fig. 2C) showed three characteristic peaks at 3429.43/cm, 2920.23/cm, and 1716.65/cm which indicate hydroxyl, carboxylic acid, and aldehyde functional groups,

respectively, while CHL spectrum (Fig. 2D) showed vibrational peaks of hydroxyl and carboxylic acid functional groups at 3417.86/cm and 2929/cm, respectively [46].

By comparing the FTIR spectra of pure SER and its physical mixtures with the excipients (Fig. 2E–H), no significant changes or shifting in the characteristic peaks of SER and different excipients were observed. Consequently, it can be deduced that there were no interactions between SER and the selected excipients proving SER-excipient compatibility.

### Analysis of Factorial Design

Eight SER-loaded bilosomal dispersions were prepared by thin film hydration method with different compositions of span 60, CHL, and SDC as proposed by  $2^3$  full factorial design according to composition shown in Table II. ANOVA (classical sum of squares — type III) for data analysis of factorial design was performed using Design-Expert® software. All the studied responses were tested for fitting to main effect, 2FI and 3FI models. The best fit model for elucidating the effect of the independent variables on responses was the one with the highest predicted  $R^2$  and the lowest PRESS (predicted residual error sum of squares) [47, 48]. Moreover, adjusted  $R^2$  and predicted  $R^2$  for the selected model should be within approximately 0.2 of each other to be in a reasonable agreement [13]. Also, the value of model adequate precision should be more than 4 to indicate adequate signal-to-noise ratio [41]. It was revealed that the 3FI model was the best fit model for the responses ( $Y_1$ ,  $Y_2$ ,  $Y_4$ ,  $Y_5$ , and  $Y_6$ ) while the main effect model was the best fit model for the response ( $Y_3$ ).

The polynomial equations in terms of coded factors were used to analyze and predict the effect of the given levels of each factor ( $X_1$ ,  $X_2$ , and  $X_3$ ), the two-factor interaction ( $X_1X_2$ ,  $X_1X_3$  and  $X_2X_3$ ), and the three-factor interaction ( $X_1X_2X_3$ ) on the responses as the following:

$$Y = \beta_0 + \beta_1X_1 + \beta_2X_2 + \beta_3X_3 + \beta_4X_1X_2 + \beta_5X_1X_3 + \beta_6X_2X_3 + \beta_7X_1X_2X_3 \quad (9)$$

where  $Y$  symbolizes the response,  $\beta_0$  is the intercept, and  $\beta_1$ – $\beta_7$  are the model terms coefficients. The terms  $X_1$ ,  $X_2$ , and  $X_3$  stand for the main effect while  $X_1X_2$ ,  $X_1X_3$ , and  $X_2X_3$  are the two-way interaction terms and show how the response changes when two factors are simultaneously changed. The term  $X_1X_2X_3$  represents three-way interaction that shows how the response changes when three factors are simultaneously changed [49]. The positive sign of the coefficient indicates a directly proportional relationship between the factor and response, whereas the negative sign indicates an inversely proportional relationship [13]. The experimental data of all responses are summarized in



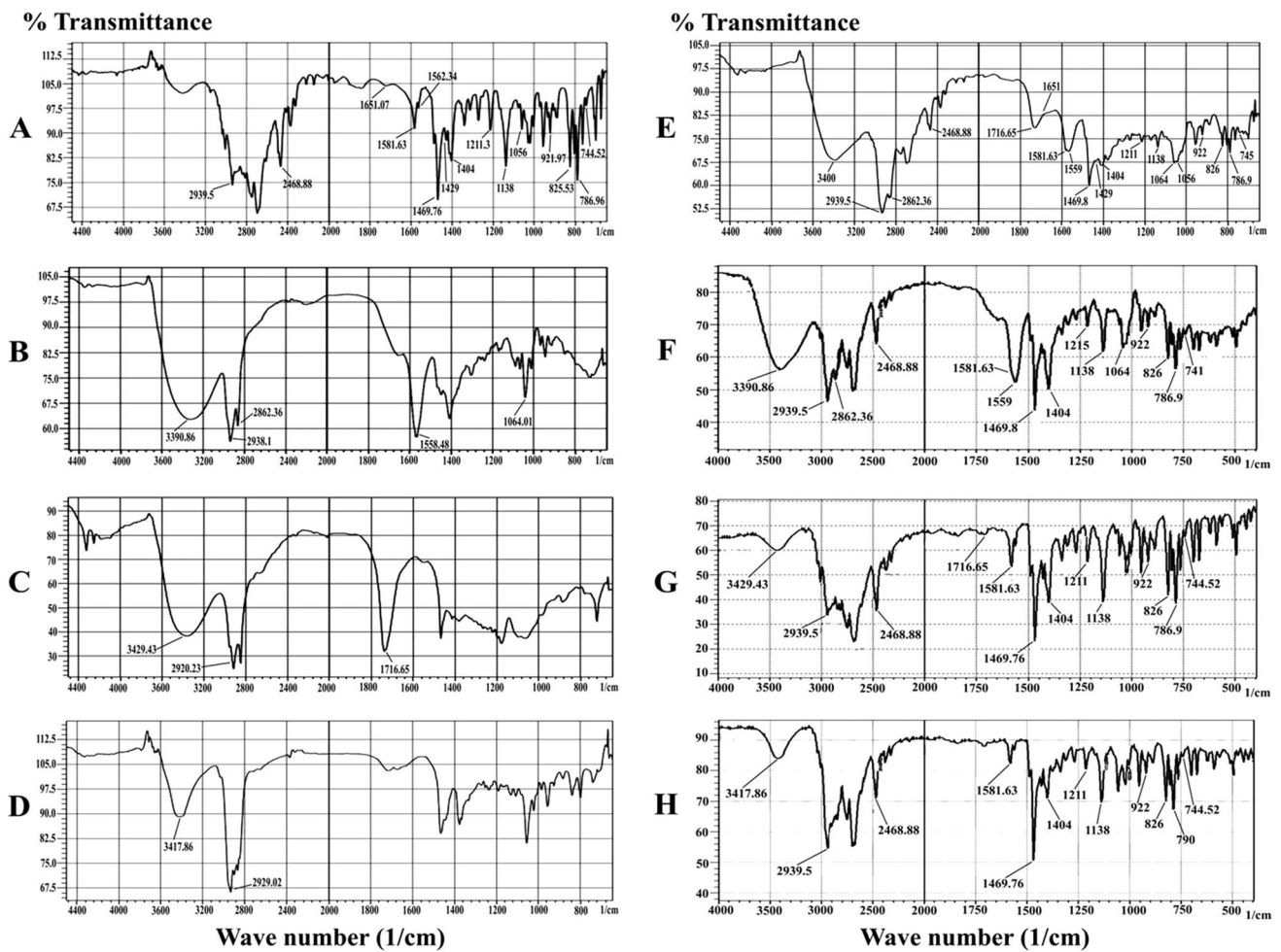


**Fig. 2** FTIR spectra of **A** SER, **B** SDC, **C** span 60, **D** CHL, **E** physical mixture (SER+SDC+span 60+CHL), **F** physical binary mixture (SER+SDC), **G** physical binary mixture (SER+span 60), and **H** physical binary mixture (SER+CHL)

**Table II** Composition of the prepared bilosomal dispersions

Formula code	$X_1$ Total conc. of span 60 and CHL (%w/v)	$X_2$ Span 60:CHL molar ratio	$X_3$ SER:SDC molar ratio	Amount (mg)			
				SER	Span 60	CHL	SDC
N1	0.5	1	0.5	50	80	70	133
N2	0.5	7	0.5	50	133	17	133
N3	1	1	0.5	50	160	140	133
N4	1	7	0.5	50	266	34	133
N5	0.5	1	0.25	50	80	70	266
N6	0.5	7	0.25	50	133	17	266
N7	1	1	0.25	50	160	140	266
N8	1	7	0.25	50	266	34	266

CHL cholesterol, SDC sodium deoxycholate, SER sertraline hydrochloride

Table III. The coefficients of all model terms emanated from polynomial equations of measured responses are shown in Table IV. The 3D response surface plots for all responses are illustrated in Fig. 3.

**Effects of Experimental Variables on EE% ( $Y_1$ )**

The EE% of SER within bilosomal formulae ranged from  $30 \pm 1.3\%$  for N5 to  $87 \pm 1.7\%$  for N4 as summarized in

Table III, which proves the successful entrapping of SER into the bilosomal vesicles and the ability of bilosomes to be a promising carrier for SER. Statistical analysis of the 3FI model using ANOVA revealed that the model terms ( $X_1$ ,  $X_2$ , and  $X_3$ ) as well as the two-factor interactions ( $X_1X_3$  and  $X_2X_3$ ) had significant impact ( $P < 0.05$ ) on  $EE\%$  ( $Y_1$ ) while the two-factor interaction ( $X_1X_2$ ) and the three-factor interaction ( $X_1X_2X_3$ ) were insignificant ( $P > 0.05$ ). The individual effect of total span 60 and CHL concentration ( $X_1$ ) was significantly positive on  $EE\%$ . Thus, increasing the total concentration from 0.5 to 1%w/v was found to increase  $EE\%$ . This result can be rationalized that increasing the concentration of bilayer-forming ingredients will definitely increase the number of the created bilosomes per unit volume and subsequently more amount of drug will be accommodated per unit volume which means higher carrying capacity [7]. Regarding span 60:CHL molar ratio ( $X_2$ ), it was observed that ( $X_2$ ) showed a significant ( $P < 0.05$ ) positive effect on  $EE\%$ . This might be attributed to the increased span 60 levels. The long alkyl chain and low hydrophilic–lipophilic balance (HLB) of span 60 could improve the  $EE\%$  by increasing the solubility and permeability of lipophilic SER into bilosomes vesicles [12, 41]. Also, CHL could compete with drug molecules for the alignment into the hydrophobic

packing spaces of the vesicles' bilayer membrane during vesicles formation in the hydration process [7, 50]. Consequently, higher amount of SER would be incorporated into the bilosomes with higher  $X_2$  level (lower cholesterol level). Previously, it was reported that increased CHL levels led to increased  $EE\%$  due to the increased hydrophobicity of the vesicles [12]. However, in this study, the effect of increasing span 60 levels was found to be more prominent.

Moreover, SER:SDC molar ratio ( $X_3$ ) affected  $EE\%$  positively. The formulae with SER:SDC molar ratio (0.5) showed higher  $EE\%$  than their corresponding formulae which have lower SER:SDC molar ratio (0.25). This is probably due to the exaggerated fluidization of the vesicles' lipid bilayers which contain greater levels of SDC (lower SER:SDC molar ratio) that can lead to drug leakage. Also, the presence of SDC in high concentrations in the bilosomal systems can induce vesicle bilayer-forming molecules to start making micelles which initially generate pores in the bilosomal membrane and cause drug leakage as a consequence; then, a complete conversion of the bilosomal membranes into mixed micelles occurs [18, 51]. The produced mixed micelles were reported to have lower drug loading capacity than its parent vesicles [52], and it will increase the water solubility of SER during the hydration process and thus the soluble SER

**Table III** Results of responses ( $EE\%$ ,  $ZP$ ,  $PS$ ,  $Q_2$ ,  $Q_8$ , and  $Q_{24}$ ) and  $PDI$  for the prepared bilosomal dispersions

Formula code	$Y_1$ $EE$ (%)	$Y_2$ $ZP$ (mW)	$Y_3$ $PS$ (nm)	$Y_4$ $Q_2$ (%)	$Y_5$ $Q_8$ (%)	$Y_6$ $Q_{24}$ (%)	$PDI$
N1	68±0.70	-41±0.78	337±19	44.81±3.46	59.50±1.42	69.57±0.86	0.544±0.09
N2	79±0.50	-37.4±0.15	251±7	36.97±0.25	40.20±0.36	44.23±0.25	0.576±0.03
N3	74±1.60	-40.5±1.6	374±23	19.67±1.00	25.60±0.60	34.70±1.49	0.552±0.05
N4	87±1.70	-40.3±0.3	306±4	18.37±1.37	24.00±1.64	29.50±1.95	0.433±0.02
N5	30±1.30	-40.6±0.6	381±35	56.23±0.91	66.03±2.07	75.50±1.35	0.617±0.1
N6	39±0.16	-36.8±2.25	302±2.6	38.47±0.45	42.03±0.06	47.27±0.21	0.440±0.009
N7	54±2.0	-41.2±1.1	474±79	48.93±0.24	55.20±0.76	66.70±0.20	0.670±0.09
N8	61±0.50	-44.5±2.39	385±41	31.07±0.31	36.67±0.49	42.30±0.30	0.737±0.024

$EE$  entrapment efficiency,  $ZP$  zeta potential,  $PS$  particle size,  $PDI$  polydispersity index

**Table IV** Values of intercept and coefficients of polynomial equations for all responses

Equation terms	Coefficients					
	$Y_1$	$Y_2$	$Y_3$	$Y_4$	$Y_5$	$Y_6$
Intercept	+61.62	+40.32	+350.89	+36.81	+43.65	+51.22
$X_1$	+7.48	+1.33	+33.00	-7.30	-8.29	-7.92
$X_2$	+4.94	-0.5417	-39.79	-5.60	-7.93	-10.40
$X_3$	+15.50	-0.4917	-33.98	-6.86	-6.33	-6.72
$X_1X_2$	+0.0633	+1.29	—	+0.8046	+2.90	+3.00
$X_1X_3$	-3.95	-0.7250	—	-3.63	-4.24	-4.48
$X_2X_3$	+0.9742	-0.4000	—	+3.31	+2.70	+2.76
$X_1X_2X_3$	+0.4833	-0.4500	—	+0.8312	+1.53	+2.04

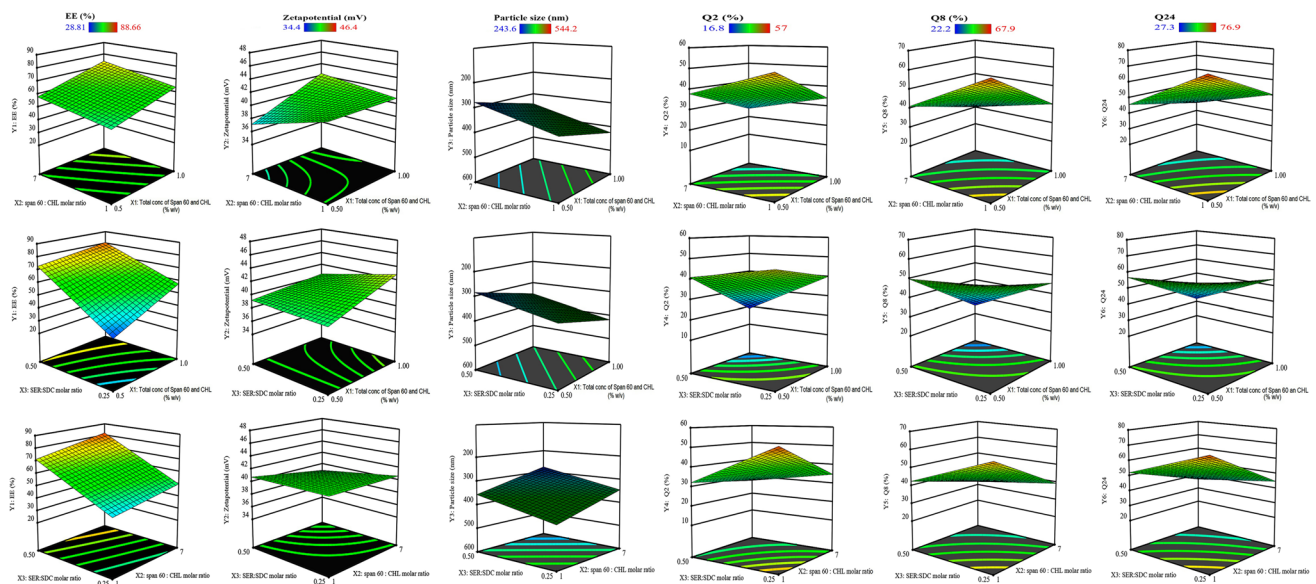


**Fig. 3** The 3D response surface plots showing the effect of independent variables on all responses

will be separated in the supernatant after centrifugation and discarded [18].

The polynomial equation revealed a significant negative  $X_1X_3$  interaction ( $P < 0.05$ ) for the response ( $Y_1$ ). Thus, the combined effect of  $X_1$  and  $X_3$  on  $Y_1$  is less than the sum of their individual effects (antagonism), whereas a significant positive  $X_2X_3$  interaction ( $P < 0.05$ ) indicated the synergism between  $X_2$  and  $X_3$ . Thus, the increase of  $X_3$  from 0.25 to 0.5 leads to more positive effect on  $EE\%$  upon increasing ( $X_2$ ) from 1 to 7.

### Effects of Experimental Variables on ZP ( $Y_2$ )

Zeta potential assessment is the most valuable technique for estimating the physical stability of vesicular dispersion against particles aggregation, enlargement, and sedimentation [53]. As shown in Table III, all of the SER-loaded bilosomes acquired zeta potential values ranged between  $-36.80$  and  $-44.50$  mV. These zeta potential values are sufficient to achieve adequate electric repulsion between vesicles to prevent their aggregation and maintain dispersion physical stability [17, 18]. Interestingly, this negative charge carried by the vesicles was reported to promote drug uptake through M-cells in the Peyer's patch and enhance the drug absorption through the intestinal lymphatic transport pathway [7, 53, 54]. Furthermore, the negative charge has a membrane-destabilizing impact that can increase the fluidity of the intestinal membrane and facilitate the transportation of the bilosomal vesicles through it [53]. Statistical analysis of the 3FI model using ANOVA revealed that the model terms  $X_1$ ,  $X_1X_2$  and  $X_1X_3$  had significant impact ( $P < 0.05$ )

on zeta potential ( $Y_2$ ), while  $X_2$ ,  $X_3$ ,  $X_2X_3$  and  $X_1X_2X_3$  were insignificant ( $P > 0.05$ ).

The individual effect of  $X_1$  was significantly positive on zeta potential ( $P < 0.05$ ). This might be attributed to increased CHL concentration which was previously reported to introduce a negative charge onto the vesicles' surface due to the uneven polarity distribution of CHL hydroxyl group [55, 56], as well as increased surfactant concentration that cause an increase in the electrical conductivity [56, 57].

The positive coefficient of  $X_1X_2$  interaction ( $P < 0.05$ ) indicated the synergistic effect of increasing  $X_2$  from 1 to 7 with the positive effect of increasing  $X_1$  from 0.5 to 1%w/v on the absolute value of zeta potential, whereas the significant negative  $X_1X_3$  interaction ( $P < 0.05$ ) indicated the antagonistic combined effect of  $X_1$  and  $X_3$  on zeta potential. As the level of  $X_3$  decreased from 0.5 to 0.25 (i.e., SDC increased), the more increase in the absolute value of zeta potential would be observed upon the increasing  $X_1$ . Thus, the incorporation of bile salt (SDC) within the bilosomal vesicular structure contributes in the appearance of negative charge on the bilosomal surface [41].

### Effects of Experimental Variables on PS( $Y_3$ )

Vesicular particle size plays an important role in the in vitro release behavior, ex vivo intestinal permeation, and in vivo intestinal absorption of the drug, as small vesicular sizes up to 400 nm can improve intestinal drug absorption as well as oral bioavailability [58, 59]. Particle size values of the prepared bilosomal formulae ranged from  $251 \pm 7$  nm for N2 to  $474 \pm 79$  nm for N7 (Table III). Statistical analysis of the main effect factorial design model using ANOVA revealed

that the model terms ( $X_1$ ,  $X_2$ , and  $X_3$ ) had significant impact ( $P < 0.05$ ) on particle size of bilosomal vesicles ( $Y_3$ ).

An increase in particle size was observed with increasing the total concentration of span 60 and CHL ( $X_1$ ) which may be due to the insufficient distribution of sonication energy in the concentrated bilosomal dispersions, and this sonication energy was accountable for reducing the vesicular size more efficiently [6]. Decreasing span 60:CHL molar ratio ( $X_2$ ) was found to increase the particle size. This could be due to the ability of high concentrations of CHL to hinder close alignment of vesicles' bilayer forming lipids resulting in increased distribution of the water within the lipid bilayer and thus increase the width of the bilayer with subsequent increase of the particle size [14, 41]. Also, decreasing SER:SDC molar ratio ( $X_3$ ) from 0.5 to 0.25 was found to produce larger bilosomal vesicles which could be attributed to the high viscosity caused by high concentration of SDC in the hydration medium, enhanced flexibility, and decreased surface tension of the vesicles [11, 53, 54]. Moreover, *PDI* values for all the prepared bilosomal formulae ranged between 0.440 and 0.737 (Table III) indicating limited particle size distribution and good homogeneity [18].

#### Effects of Experimental Variables on % SER Released at 2, 8, and 24 h ( $Y_4$ , $Y_5$ , and $Y_6$ , Respectively)

The release profiles of SER from the prepared bilosomal dispersions are illustrated in Fig. 4. The cumulative % SER released after 24 h ( $Q_{24}$ ) from all the prepared bilosomal dispersions were ranged from  $29.5 \pm 1.95\%$  for N4 to  $75.50 \pm 1.35\%$  for N5 (Table III). The release profiles of all formulae exhibited a biphasic release pattern; a primary rapid release phase extended up to approximately 2 h, followed by a slower release phase. The prompt release that occurred at the beginning might be attributed to the liberation of SER molecules adsorbed on the outer most surface of the bilosomal vesicles in addition to the diffusion of the other molecules located in the outer vesicles' membrane directly into the release medium. Subsequently, SER molecules in the sequential inner layers diffuse to the neighboring outer layers towards the surface of the vesicle and then to the release medium which is a time-consuming and retardable process resulting in the secondary sustained release phase [7, 19].

Statistical analysis of the 3FI factorial design model using ANOVA revealed that the model main factors ( $X_1$ ,  $X_2$ , and  $X_3$ ), the two-factor interaction ( $X_1X_2$ ,  $X_1X_3$ , and  $X_2X_3$ ), and the three-factor interaction ( $X_1X_2X_3$ ) had significant impact ( $P < 0.05$ ) on the cumulative % drug released at 2 h  $Q_2$  ( $Y_4$ ), 8 h  $Q_8$  ( $Y_5$ ), and 24 h  $Q_{24}$  ( $Y_6$ ).

All investigated formulation variables ( $X_1$ ,  $X_2$ , and  $X_3$ ) had negative coefficients, indicating the inversely proportional relationship with the cumulative % drug released at 2, 8, and 24 h. The negative effect of increasing the total concentration

of span 60 and CHL ( $X_1$ ) from 0.5 to 1% (w/v) on SER release from bilosomal vesicles might be attributed to the stiffer solidified nano-vesicles and the higher medium viscosity caused by the higher concentration of lipids [60]. The negative effect of changing span 60:CHL molar ratio ( $X_2$ ) from 1 to 7 on SER release might be due to increasing span 60 levels in the bilosomal vesicles' assembly. Span 60 has a low hydrophilic-lipophilic balance (HLB value = 4.7) and a very long saturated alkyl chain (stearate moiety = C18); thus, there is a high structural affinity between the hydrophobic SER and the stearate moiety of span 60. Also, span 60 has a high glass transition temperature ( $T_g = 58^\circ\text{C}$ ) which may account for producing very stable and firm bilayer membranes that retard the drug leakage. Briefly, higher span 60 ratios in the bilosomal vesicles' structure show higher SER affinity and retard its diffusion to the release medium [19, 61]. The negative effect of changing SER:SDC molar ratio ( $X_3$ ) from 0.25 to 0.5 is possibly due to the decreased micelle formation and fluidization of the bilosomal lipid bilayer due to decrease in SDC concentration [51, 54]. Regarding the two factor interactions, there were significant positive effects ( $P < 0.05$ ) of ( $X_1X_2$ ) and ( $X_2X_3$ ) interactions on the responses ( $Y_4$ ,  $Y_5$ , and  $Y_6$ ), whereas ( $X_1X_3$ ) interaction had a significant negative effect ( $P < 0.05$ ). Moreover, the three factor interaction ( $X_1X_2X_3$ ) exhibited significant positive effect ( $P < 0.05$ ) for the responses ( $Y_4$ ,  $Y_5$ , and  $Y_6$ ).

#### Release Kinetics and Mechanisms

The in vitro release data obtained from the bilosomal formulae were best fitted to the diffusion-controlled release model (Higuchi's equation) as indicated from the highest correlation coefficients ( $R^2$ ) [23]. Moreover, when the data processed with Korsmeyer and Peppas model, bilosomal formulae (N1, N2, N3, N4, N6, and N8) exhibited exponent  $n$

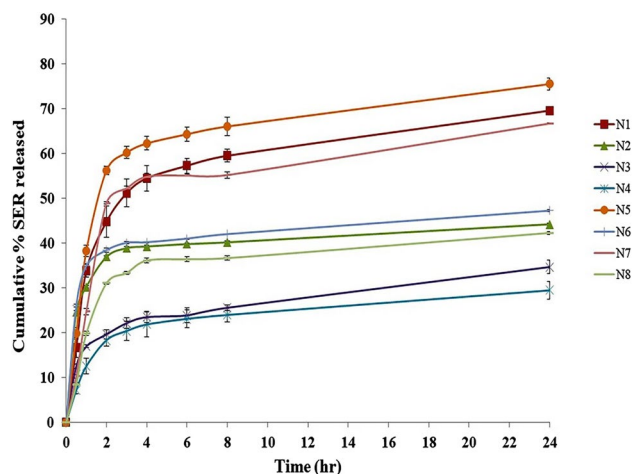


**Fig. 4** In vitro release profiles of SER from the prepared bilosomal dispersions

value less than 0.45 demonstrating Fickian diffusion release mechanism, while bilosomal formulae (N5 and N7) exhibited exponent  $n$  value more than 0.45 and less than 0.89 demonstrating the non-Fickian anomalous transport mechanism, i.e., the drug release was governed by more than one process (diffusion and erosion mechanism) [23, 28].

### Optimization of SER-Loaded Bilosomal Dispersions

The optimization was carried out using numerical optimization technique based on desirability approach. According to the constraints provided in Table I, Design-Expert® software revealed that N1 was the optimum formula that could satisfy most of the required constraints with the highest desirability value of 0.657. The optimum formula N1 was validated by comparing its experimental responses values with its predicted response values. The percentage deviation for each response was determined and was calculated as follows:

$$\% \text{deviation} = \frac{|\text{Predicted value} - \text{Experimental value}|}{\text{Predicted value}} \times 100 \quad (10)$$

The % deviation for all responses did not exceed 4.11% as shown in Table V.

### TEM

TEM photograph of the optimal bilosomal dispersion (N1) in Fig. 5 revealed that bilosomal vesicles were dispersed as non-aggregated individual particles with a predominant nano-sized spherical shape and well-defined core and outline.

### Preparation of SER-Loaded Bilosomal Powder

The main stability issues with nano-vesicle formulations are fusion, aggregation, swelling, and drug leakage. In order to improve their stability, it is recommended to store them in the dry powder form instead of their aqueous dispersion form. Indeed, freeze-drying technique has proven to be an effective method for long-term storage of these formulations in previous studies [62, 63]. Hence, bilosomes in powdered form are superior to traditional liquid form in respect of convenience of storage, transport, dosing, tableting, and capsule filling [15]. The selected optimal bilosomal dispersion (N1) was freeze dried to produce FDN1 powder and stored in a desiccator at 25°C for further studies.

### Determination of Drug Loading (%) in Freeze-Dried Bilosomal Powder

The % SER-loaded in the bilosomal powder (FDN1) was found to be  $15.43 \pm 0.91\%$  w/w. This result was not

significantly different ( $P > 0.05$ ) from the % drug loading of the non-lyophilized form (N1) which was  $11.66 \pm 2.36\%$ .

Moreover, comparing  $EE\%$  before and after lyophilization of the optimized formula showed no significant difference ( $P > 0.05$ ). The  $EE\%$  was  $68.24 \pm 0.7\%$  and  $67.90 \pm 3.99\%$  for the non lyophilized form (N1) and the lyophilized form (FDN1), respectively.

### In Vitro Release from the Freeze-Dried Bilosomal Powder

The cumulative release profiles of SER from the bilosomal powder (FDN1) and pure SER are illustrated in Fig. 6. It could be noticed that a complete dissolution of pure SER was achieved within 10 h, whereas a remarkable sustained release up to 24 h from FDN1 bilosomes was observed. Within the first 2 h,  $82.49 \pm 6.11\%$  of pure SER was dissolved while FDN1 showed only  $23.75 \pm 0.58\%$  drug released. The high percentage dissolved of pure SER within the first 2 h in the SGF release medium could be the main reason for the side effects of SER in the upper GIT due to the direct contact with stomach. Also, thick mucus layer and short transit time of the stomach might hinder drug released in stomach and limit its absorption process. Thus, minimizing the gastric exposure by sustaining the release of SER as achieved from bilosomal powder (FDN1) is advantageous [5, 64]. Due to the basic nature of SER and pH-dependent solubility, the majority of the un-absorbed SER dissolved in the stomach might be converted to free base form when enter the intestinal region leading to particle aggregation in the alkaline intestinal medium resulting in poor or slow release and further poor absorption and low bioavailability [3, 4]. However, it was found that the total SER released from the prepared bilosomal powder (FDN1) in SIF was 66.82% compared to 17.51% only of pure SER dissolved. Hence, the vast majority of SER was released from FDN1 in SIF medium and the drug released in the intestinal region would be subjected to more efficient absorption due to the large

**Table V** Validation of the optimized SER-loaded bilosomal dispersion (N1)

Response	Predicted value	Experimental value	% Error
$EE\%$	68.23	68.00	0.34%
Zeta potential	41.00*	41.00*	0.00%
Particle size	323.70	337.00	4.11%
$Q_2$	44.81	44.81	0.00%
$Q_8$	59.50	59.50	0.00%
$Q_{24}$	69.57	69.57	0.00%

$EE\%$  entrapment efficiency

\*Absolute value of zeta potential

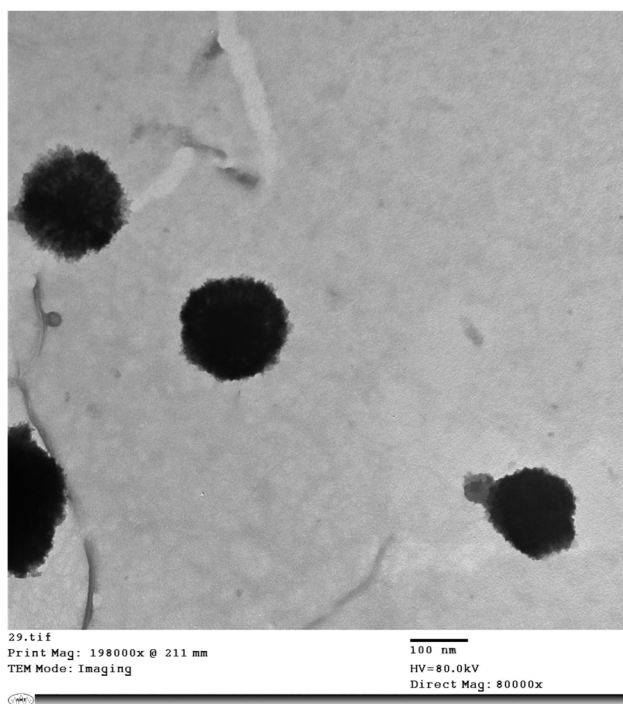


**Fig. 5** Transmission electron microscope photograph of the optimal bilosomal dispersion (N1)

surface area, good permeability and long transit time of the intestine [64]. The solubilizing effect of bilosomes helped to maintain the drug into the solubilized state throughout its release in the alkaline SIF medium. Also, the particle size of the bilosomal vesicles provided larger surface area exposed to the release medium in case of FDN1 and thus permitting higher rate of drug release in the intestinal medium [7, 63].

The *in vitro* release data of FDN1 were best fitted to the diffusion-controlled release model (Higuchi's equation) as indicated from the highest correlation coefficient ( $R^2 = 0.9919$ ). Moreover, when the data processed with Korsmeyer-Peppas model, FDN1 exhibited exponent  $n$  value equals to 0.715 demonstrating the non-Fickian anomalous transport mechanism [12, 23, 28].

### Studies of Storage Effect on Bilosomal Powder (FDN1)

The average zeta potential ( $ZP$ ), particle size ( $PS$ ),  $PDI$ , % drug loading, and dissolution efficiency ( $DE\%$ ) were evaluated at (0, 1, and 3 months) (Table VI). The demonstrated data showed that there was no significant difference ( $P < 0.05$ ) between the values of  $ZP$ ,  $PS$ ,  $PDI$ , % drug loading, and  $DE\%$  at 2, 8, and 24 h at zero time and the values of such parameters after 1 and 3 months' storage. These results can prove the stability of the lyophilized bilosomal powder FDN1 at room temperature. Interestingly, it was noticed

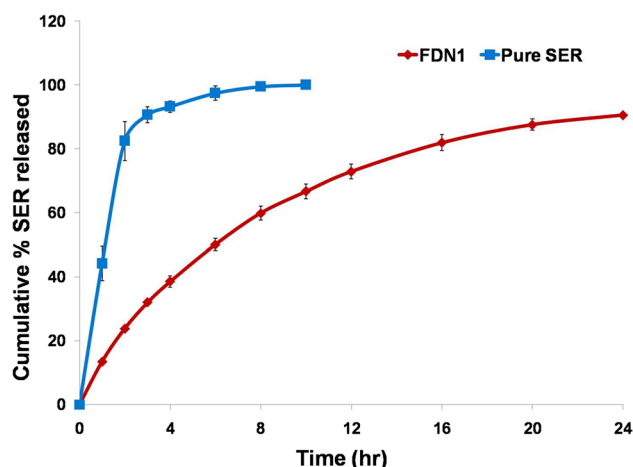


**Fig. 6** *In vitro* release profiles of SER from the bilosomal powder (FDN1) versus pure SER

that the particle size of bilosomes was decreased upon lyophilization from  $337 \pm 19$  nm for N1 to  $184.17 \pm 10.6$  nm for FDN1. This notice comes in agreement with a previous study by Shokri et al. [65].

### HPLC Assay of SER

The described HPLC assay showed good linearity in the range of SER concentration (10–200  $\mu\text{g/ml}$ ) with regression coefficient ( $R^2 = 0.999$ ). The peak of the drug was sharp and symmetric with good baseline and minimal tailing at retention time of 3.449 min. The assay was proved to be sensitive, accurate, and reproducible. The mean % recovery for intra- and inter-quality control samples ranged from 99.50 to 101.41% reflecting high accuracy of the assay. Also,  $RSD\%$  of all intra- and inter-quality control samples were less than 2% indicating a high degree of intra- and inter-day precisions of the assay.

### Ex Vivo Drug Permeation Study

The gut permeation study was performed on a rabbit intestine to calculate the intestinal permeation efficiency of SER from FDN1 compared to the pure SER. The displayed permeation profiles (Fig. 7) distinctly confirmed the potential of the bilosomal delivery system to improve SER permeation through GIT membrane.

The permeation flux value was found to be  $150.43 \mu\text{g}/\text{cm}^2/\text{h}$  and  $29.52 \mu\text{g}/\text{cm}^2/\text{h}$  for FDN1 and pure SER, respectively. Consequently, the apparent permeability coefficient ( $APC$ ) of FDN1 was found to be  $4.2 \times 10^{-2} \text{ cm/h}$  which is markedly higher compared to pure SER that showed  $APC$  of  $8.3 \times 10^{-3} \text{ cm/h}$ . The permeation enhancement ratio ( $ER$ ) of FDN1 showed fivefold increment in the permeation of the drug. This permeation improvement is ascribed to the

**Table VI** Storage effect on FDN1 powder for 3 months

Time of storage (month)	ZP (mV)	PS (nm)	PDI	Drug loading (%w/w)	DE% at 2 h	DE% at 8 h	DE% at 24 h
0	-28.23 ± 7.62	184.17 ± 10.6	0.393 ± 0.023	15.43 ± 0.91	12.65 ± 0.395	35.86 ± 1.003	64.91 ± 1.61
1	-31.53 ± 3.84	252.07 ± 81	0.483 ± 0.066	15.37 ± 0.93	12.46 ± 0.235	35.95 ± 0.392	64.75 ± 0.49
3	-28.40 ± 1.61	271.57 ± 74.46	0.506 ± 0.059	15.40 ± 1.06	12.75 ± 0.476	36.47 ± 0.931	64.25 ± 0.448

DE% dissolution efficiency %, ZP zeta potential, PS particle size, PDI polydispersity index

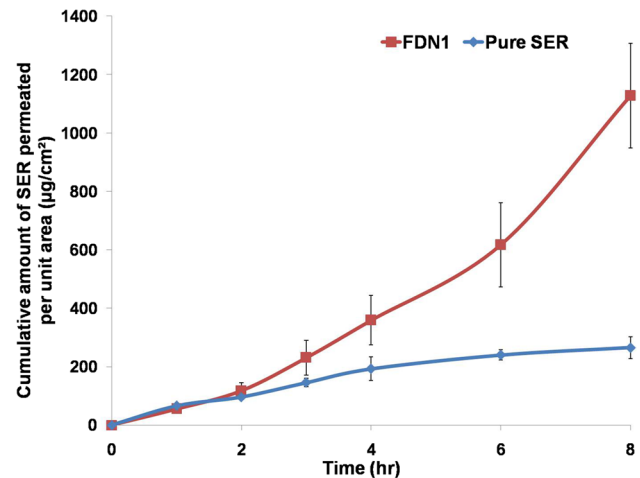
nano-sized bilosomal vesicles and the successful internalization of SER into these vesicles containing SDC bile salts. It has been reported that bile salts give an elastic property to the vesicles and serve as permeability enhancers due to its negative charge which has a membrane-destabilizing effect that increase the fluidity of biological barriers including the intestinal membrane and thus facilitate the drug diffusion and penetration across it. Moreover, the negative charge of the vesicles was previously mentioned to promote drug uptake through intestinal M-cells and enhance the drug absorption through the intestinal lymphatic transport pathway [7, 13, 53].

Furthermore, the presence of non-ionic surfactant also enhances the permeation capacity by providing a hydrostatic pressure that opens the tight junctions of the intestinal membrane, reducing the reticulo-endothelial uptake, and also inhibiting the P-gp efflux pump present in the enterocytes villus tip of the gastrointestinal tract in order to mitigate the drug pumping back into the intestinal lumen [12, 33].

### In Vivo Absorption Study

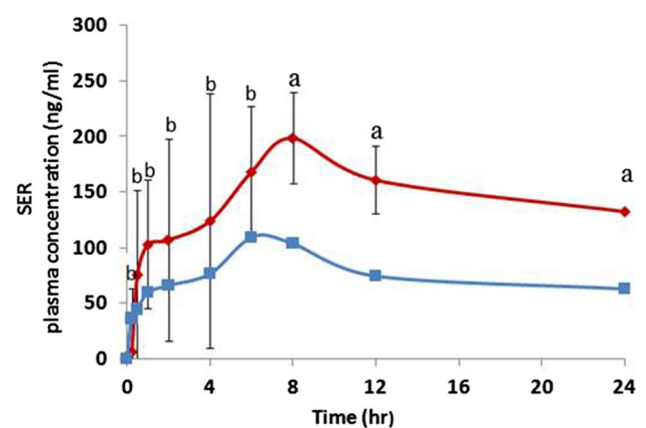
The described liquid chromatography–mass spectrometry assay had a good linearity from 0.5 to 100 ng/ml with correlation coefficient of  $R^2 = 0.9991$ . Both SER and loperamide hydrochloride showed sharp symmetric peaks with good baseline at retention time 0.397 and 0.390 min, respectively. The assay was proved to be sensitive, accurate, and reproducible. The mean % recovery for intra- and inter-quality control samples ranged from 97.03 to 104.05% reflecting high accuracy of the assay. Also, RSD% of all intra- and inter-quality control samples were less than 6% indicating a high degree of intra- and inter-day precisions of the assay.

Figure 8 shows the profiles of the mean plasma concentrations of orally administered SER from the investigated formula (FDN1) and the pure drug as a function of time. The mean values of  $C_{p,max}$  were  $201.52 \pm 63.99$  and  $112.93 \pm 7.98$  ng/ml and  $AUC_{0-24}$  were  $3848.29 \pm 889.76$  and  $1733.06 \pm 404.56$  ng h/ml, for FDN1 and pure SER, respectively. The median values of  $T_{max}$  following administration of FDN1 and pure SER were 8 h and 6 h, with interquartile range (IQR) of 6 and 1, respectively. The difference between the  $C_{p,max}$  and  $AUC_{0-24}$  values of both



**Fig. 7** Permeability behaviors of SER from the bilosomal powder (FDN1) versus pure SER

FDN1 formulation and pure SER was statistically significant ( $P < 0.05$ ). Regarding the  $T_{max}$ , the non-parametric Mann–Whitney test verified that  $T_{max}$  was insignificantly different at  $P < 0.05$ .



**Fig. 8** SER plasma concentration–time curves after oral administration of single dose (11.16 mg/kg) of the investigated freeze-dried SER-loaded bilosomal powder (FDN1) and pure SER over 24 h. Each data point represents mean  $\pm$  SD ( $n = 5$ ). **a** Significantly different ( $P < 0.05$ ) from pure SER. **b** Not significantly different ( $P > 0.05$ ) from pure SER

The mean  $C_{p_{max}}$  and  $AUC_{0-24}$  in the group administered FDN1 was 1.78- and 2.22-fold higher than the group administered the pure SER, respectively. Consequently, the relative bioavailability % ( $Fr$  %) of FDN1 formulation compared to pure SER was found to be 222% based on  $AUC_{0-24}$ . This improvement in the oral bioavailability of SER from bilosomal powder (FDN1) could be attributed to the successful entrapment of SER into the nano-sized bilosomal vesicles that composed mainly of the surfactant (span 60) which has a solubilizing effect and acts as penetration enhancer. Moreover, bilosomal vesicles included bile salts which give an elastic property to the vesicles, serve as permeability enhancers, and make vesicles resistant to physiological bile salts in the GIT. Also, the negative charge of the vesicles promotes drug uptake through intestinal M-cells of Peyer's patch and enhances the drug absorption through the intestinal lymphatic transport pathway, thus escaping the hepatic first-pass metabolism [7, 12, 13].

## Conclusion

In this study, SER-loaded bilosomal formula (0.5% w/v span 60 and CHL, span 60-to-CHL molar ratio = 1, SER-to-SDC molar ratio = 0.5) was selected as optimal system with acceptable entrapment efficiency, zeta potential, particle size,  $PDI$ , and remarkable sustained in vitro drug release over 24 h with minimized release at 2 h. The lyophilized optimal bilosomal system exhibited good stability upon storage for 3 months at ambient conditions and achieved fivefold higher SER permeation efficiency through rabbit intestinal membrane compared to pure SER. In vivo absorption studies in rats revealed relative bioavailability % ( $Fr$  %) of 222% for SER-loaded bilosomal powder (FDN1) compared to pure SER. Therefore, the developed SER bilosomal system is promising for oral administration of SER in order to improve its oral bioavailability with reducing gastric upset.

**Supplementary Information** The online version contains supplementary material available at <https://doi.org/10.1208/s12249-022-02339-0>.

**Author Contribution** Aliaa Ismail: conceptualization, factorial design, data formal analysis, writing—review and editing. Mohammed Teiama: conceptualization, data interpretation, writing—review and editing. Basma Magdy: carrying out experiments, data interpretation, and writing—original draft preparation. Wedad Sakran: conceptualization, supervision, and review. All authors have read and approved the manuscript for publication.

**Funding** Open access funding provided by The Science, Technology & Innovation Funding Authority (STDF) in cooperation with The Egyptian Knowledge Bank (EKB).

## Declarations

**Conflict of Interest** The authors declare no competing interests.

**Open Access** This article is licensed under a Creative Commons Attribution 4.0 International License, which permits use, sharing, adaptation, distribution and reproduction in any medium or format, as long as you give appropriate credit to the original author(s) and the source, provide a link to the Creative Commons licence, and indicate if changes were made. The images or other third party material in this article are included in the article's Creative Commons licence, unless indicated otherwise in a credit line to the material. If material is not included in the article's Creative Commons licence and your intended use is not permitted by statutory regulation or exceeds the permitted use, you will need to obtain permission directly from the copyright holder. To view a copy of this licence, visit <http://creativecommons.org/licenses/by/4.0/>.

## References

1. Singh HK, Saadabadi A. Sertraline. StatPearls. Treasure Island (FL): StatPearls Publishing; 2021. <http://www.ncbi.nlm.nih.gov/pubmed/31613469>
2. Abouhusein DMN, El Nabarawi MA, Shalaby SH, El-Bary AA. Sertraline- cyclodextrin complex orodispersible sublingual tablet: optimization, stability, and pharmacokinetics. J Pharm Innov. 2021;16(1):53–66.
3. Rahman MA, Iqbal Z, Hussain A. Formulation optimization and in vitro characterization of sertraline loaded self-nanoemulsifying drug delivery system (SNEDDS) for oral administration. J Pharm Investig. 2012 Aug 29;42(4):191–202.
4. Al-nimry SS, Jaber MA. Preparation and optimization of sertraline hydrochloride tablets with improved dissolution through crystal modification. AAPS PharmSciTech. 2017;18(4):1190–202.
5. Uppala P, Shaik S, Valluru S, Nalluri B. Development of enteric coated sustained release matrix tablets of sertraline hydrochloride. J Appl Pharm Sci. 2015;5(04):058–64.
6. Rahman MA, Harwansh RK, Iqbal Z. Systematic development of sertraline loaded solid lipid nanoparticle (SLN) by emulsification-ultrasonication method and pharmacokinetic study in Sprague-Dawley rats. Pharm Nanotechnol. 2019 Jun 10;7(2):162–76.
7. Arzani G, Haeri A, Daeihamed M, Bakhtiari-Kaboutaraki H, Dadashzadeh S. Niosomal carriers enhance oral bioavailability of carvedilol: effects of bile salt-enriched vesicles and carrier surface charge. Int J Nanomedicine. 2015 Jul;10:4797–813.
8. Cai Z, Wang Y, Zhu L-J, Liu Z-Q. Nanocarriers: a general strategy for enhancement of oral bioavailability of poorly absorbed or pre-systemically metabolized drugs. Curr Drug Metab. 2010 Feb;11(2):197–207.
9. Nishioka Y, Yoshino H. Lymphatic targeting with nanoparticulate system. Adv Drug Deliv Rev. 2001 Mar 23;47(1):55–64.
10. Zhang L, Wang S, Zhang M, Sun J. Nanocarriers for oral drug delivery. J Drug Target. 2013 Jul;21(6):515–27.
11. Rajput T, Chauhan MK. Bilosome: a bile salt based novel carrier system gaining interest in pharmaceutical research. J Drug Deliv Ther. 2017 Sep 15;7(5):4–16.
12. Zafar A, Alruwaili NK, Imam SS, Hadal Alotaibi N, Alharbi KS, Afzal M, et al. Bioactive apigenin loaded oral nano bilosomes: formulation optimization to preclinical assessment. Saudi Pharm J. 2021;29(3):269–79. <https://doi.org/10.1016/j.jsps.2021.02.003>.



13. Saifi Z, Rizwanullah M, Mir SR, Amin S. Bilosomes nanocarriers for improved oral bioavailability of acyclovir: a complete characterization through in vitro, ex-vivo and in vivo assessment. *J Drug Deliv Sci Technol*. 2020 Jun;57: 101634. <https://doi.org/10.1016/j.jddst.2020.101634>.
14. Mohsen AM, Asfour MH, Salama AAA. Improved hepatoprotective activity of silymarin via encapsulation in the novel vesicular nanosystem bilosomes. *Drug Dev Ind Pharm*. 2017;43(12):2043–54. <https://doi.org/10.1080/03639045.2017.1361968>.
15. Jin Y, Wen J, Garg S, Liu D, Zhou Y, Teng L, et al. Development of a novel niosomal system for oral delivery of Ginkgo biloba extract. *Int J Nanomedicine*. 2013;8:421–30.
16. Rudra A, Deepa RM, Ghosh MK, Ghosh S, Mukherjee B. Doxorubicin-loaded phosphatidylethanolamine-conjugated nanoliposomes: in vitro characterization and their accumulation in liver, kidneys, and lungs in rats. *Int J Nanomedicine*. 2010;5(1):811–23.
17. Dai Y, Zhou R, Liu L, Lu Y, Qi J, Wu W. Liposomes containing bile salts as novel ocular delivery systems for tacrolimus (FK506): in vitro characterization and improved corneal permeation. *Int J Nanomedicine*. 2013;8:1921–33.
18. Ammar HO, Mohamed MI, Tadros MI, Fouly AA. Transdermal delivery of ondansetron hydrochloride via bilosomal systems: in vitro, ex vivo, and in vivo characterization studies. *AAPS PharmSciTech*. 2018;19(5):2276–87.
19. Shaker DS, Shaker MA, Hanafy MS. Cellular uptake, cytotoxicity and in-vivo evaluation of Tamoxifen citrate loaded niosomes. *Int J Pharm*. 2015;493(1–2):285–94. <https://doi.org/10.1016/j.ijpharm.2015.07.041>.
20. Jadon PS, Gajbhiye V, Jadon RS, Gajbhiye KR, Ganesh N. Enhanced oral bioavailability of griseofulvin via niosomes. *AAPS PharmSciTech*. 2009;10(4):1186–92.
21. Khan MI, Madni A, Peltonen L. Development and in-vitro characterization of sorbitan monolaurate and poloxamer 184 based niosomes for oral delivery of diacerein. *Eur J Pharm Sci*. 2016 Dec;1(95):88–95. <https://doi.org/10.1016/j.ejps.2016.09.002>.
22. Song S, Tian B, Chen F, Zhang W, Pan Y, Zhang Q, et al. Potentials of proniosomes for improving the oral bioavailability of poorly water-soluble drugs. *Drug Dev Ind Pharm*. 2015;41(1):51–62.
23. Dash S, Murthy PN, Nath L, Chowdhury P. Kinetic modeling on drug release from controlled drug delivery systems. *Acta Pol Pharm*. 2010;67(3):217–23.
24. Korsmeyer RW, Gurny R, Doelker E, Buri P, Peppas NA. Mechanisms of solute release from porous hydrophilic polymers. *Int J Pharm*. 1983;15(1):25–35.
25. Ferreira LS, Chaves MA, Dacanal GC, Pinho SC. Wet agglomeration by high shear of binary mixtures of curcumin-loaded lyophilized liposomes and cornstarch: powder characterization and incorporation in cakes. *Food Biosci*. 2018;25(August):74–82. <https://doi.org/10.1016/j.fbio.2018.08.003>.
26. Marín D, Alemán A, Montero P, Gómez-Guillén MC. Encapsulation of food waste compounds in soy phosphatidylcholine liposomes: effect of freeze-drying, storage stability and functional aptitude. *J Food Eng*. 2018;223:132–43.
27. Judefeind A, de Villiers MM. Drug loading into and in vitro release from nanosized drug delivery systems. In: *Nanotechnology in drug delivery*. New York, NY: Springer New York; 2009. p. 129–62.
28. Kamboj S, Saini V, Bala S. Formulation and characterization of drug loaded nonionic surfactant vesicles (niosomes) for oral bioavailability enhancement. *Sci World J*. 2014;2014.
29. Khan k. A. The concept of dissolution efficiency. *J Pharm Pharmacol*. 1975 Jan 12;27(1):48–9.
30. Harbi I, Aljaeid B, El-Say KM, Zidan AS. Glycosylated sertraline-loaded liposomes for brain targeting: QbD study of formulation variabilities and brain transport. *AAPS PharmSciTech*. 2016;17(6):1404–20. <https://doi.org/10.1208/s12249-016-0481-7>.
31. El-Leithy ES, Abdel-Rashid RS. Lipid nanocarriers for tamoxifen citrate/coenzyme Q10 dual delivery. *J Drug Deliv Sci Technol*. 2017;41:239–50. <https://doi.org/10.1016/j.jddst.2017.07.020>.
32. Boseila AA, Abdel-Reheem AY, Basalious EB. Design of bile-based vesicles (BBVs) for hepatocytes specific delivery of daclatasvir: comparison of ex-vivo transenterocytic transport, in-vitro protein adsorption resistance and HepG2 cellular uptake of charged and  $\beta$ -sitosterol decorated vesicles. *PLoS ONE*. 2019;14(7):1–19.
33. Neupane YR, Srivastava M, Ahmad N, Kumar N, Bhatnagar A, Kohli K. Lipid based nanocarrier system for the potential oral delivery of decitabine: formulation design, characterization, ex vivo, and in vivo assessment. *Int J Pharm*. 2014;477(1–2):601–12. <https://doi.org/10.1016/j.ijpharm.2014.11.001>.
34. Rao MT, Rao YS, Vijaya Ratna J, Kamala Kumari PV. Characterization and ex vivo studies of nanoparticle incorporated transdermal patch of itraconazole. *Indian J Pharm Sci*. 2020;82(5):799–808.
35. Melis V, Usach I, Peris JE. Determination of sertraline in rat plasma by HPLC and fluorescence detection and its application to in vivo pharmacokinetic studies. *J Sep Sci*. 2012;35(23):3302–7.
36. Nair A, Jacob S. A simple practice guide for dose conversion between animals and human. *J Basic Clin Pharm*. 2016;7(2):27.
37. Zhang M, Gao F, Cui X, Zhang Y, Sun Y, Gu J. Development and validation of an improved method for the quantitation of sertraline in human plasma using LC-MS-MS and its application to bioequivalence studies. *J Chromatogr Sci*. 2011 Feb;49(2):89–93.
38. Jain DS, Sanyal M, Subbaiah G, Pande UC, Shrivastav P. Rapid and sensitive method for the determination of sertraline in human plasma using liquid chromatography–tandem mass spectrometry (LC–MS/MS). *J Chromatogr B*. 2005 Dec;829(1–2):69–74.
39. Ghaderi F, Nemati M, Siahi-Shadbad MR, Valizadeh H, Monajjemzadeh F. Physicochemical analysis and nonisothermal kinetic study of sertraline–lactose binary mixtures. *J Food Drug Anal*. 2017;25(3):709–16. <https://doi.org/10.1016/j.jfda.2016.08.003>.
40. Johnson BM, Chang P-TL. Sertraline hydrochloride. In: *Analytical profiles of drug substances and excipients*. 1996. p. 443–86.
41. Al-Mahallawi AM, Abdelbary AA, Aburahma MH. Investigating the potential of employing bilosomes as a novel vesicular carrier for transdermal delivery of tenoxicam. *Int J Pharm*. 2015;485(1–2):329–40. <https://doi.org/10.1016/j.ijpharm.2015.03.033>.
42. Suzuki H, Ogawa M, Hironaka K, Ito K, Sunada H. A nifedipine coground mixture with sodium deoxycholate. I. Colloidal particle formation and solid-state analysis. *Drug Dev Ind Pharm*. 2001 Jan 1;27(9):943–9.
43. Elsayed I, Abdelbary AA, Elshafeey AH. Nanosizing of a poorly soluble drug: technique optimization, factorial analysis, and pharmacokinetic study in healthy human volunteers. *Int J Nanomedicine*. 2014;9(1):2943–53.
44. Bright A, Renuga Devi TS, Gunasekaran S. Qualitative and quantitative analysis of antipsychotic drugs—a spectroscopic study. *Asian J Chem*. 2010;22(8):5871–82.
45. Abdellatif MM, Khalil IA, Khalil MAF. Sertaconazole nitrate loaded nanovesicular systems for targeting skin fungal infection: in-vitro, ex-vivo and in-vivo evaluation. *Int J Pharm*. 2017;527(1–2):1–11. <https://doi.org/10.1016/j.ijpharm.2017.05.029>.
46. Ur Rehman M, Rasul A, Khan MI, Hanif M, Aamir MN, Waqas MK, et al. Development of niosomal formulations loaded with cyclosporine a and evaluation of its compatibility. *Trop J Pharm Res*. 2018;17(8):1457–64.
47. Alhakamy NA, Caruso G, Al-Rabia MW, Badr-Eldin SM, Aldawari HM, Asfour HZ, et al. Piceatannol-loaded bilosome-stabilized

- zein protein exhibits enhanced cytostatic and apoptotic activities in lung cancer cells. *Pharmaceutics*. 2021;13(5).
48. Huang Y Bin, Tsai YH, Yang WC, Chang JS, Wu PC, Takayama K. Once-daily propranolol extended-release tablet dosage form: formulation design and in vitro/in vivo investigation. *Eur J Pharm Biopharm*. 2004;58(3):607–14.
  49. Singh J, Philip AK, Pathak K. Optimization studies on design and evaluation of orodispersible pediatric formulation of indomethacin. *AAPS PharmSciTech*. 2008;9(1):60–6.
  50. Deniz A, Sade A, Severcan F, Keskin D, Tezcaner A, Banerjee S. Celecoxib-loaded liposomes: effect of cholesterol on encapsulation and in vitro release characteristics. *Biosci Rep*. 2010;30(5):365–73.
  51. Pavlović N, Goločorbin-Kon S, Danić M, Stanimirov B, Al-Salami H, Stankov K, et al. Bile acids and their derivatives as potential modifiers of drug release and pharmacokinetic profiles. *Front Pharmacol*. 2018;9(NOV):1–23.
  52. Gupta A, Aggarwal G, Singla S, Arora R. Transfersomes: A novel vesicular carrier for enhanced transdermal delivery of sertraline: development, characterization, and performance evaluation. *Sci Pharm*. 2012;80(4):1061–80.
  53. Aburahma MH. Bile salts-containing vesicles: promising pharmaceutical carriers for oral delivery of poorly water-soluble drugs and peptide/protein-based therapeutics or vaccines. *Drug Deliv*. 2016;23(6):1847–67.
  54. Chen Y, Lu Y, Chen J, Lai J, Sun J, Hu F, et al. Enhanced bioavailability of the poorly water-soluble drug fenofibrate by using liposomes containing a bile salt. *Int J Pharm*. 2009;376(1–2):153–60.
  55. Farmoudeh A, Akbari J, Saeedi M, Ghasemi M, Asemi N, Nokhodchi A. Methylene blue-loaded niosome: preparation, physico-chemical characterization, and in vivo wound healing assessment. *Drug Deliv Transl Res*. 2020;10(5):1428–41.
  56. Owodeha-Ashaka K, Ilomuanya MO, Iyire A. Evaluation of sonication on stability-indicating properties of optimized pilocarpine hydrochloride-loaded niosomes in ocular drug delivery. *Prog Biomater*. 2021;10(3):207–20. <https://doi.org/10.1007/s40204-021-00164-5>.
  57. Dukhin AS, Goetz PJ. How non-ionic “electrically neutral” surfactants enhance electrical conductivity and ion stability in non-polar liquids. *J Electroanal Chem*. 2006;588(1):44–50.
  58. Obinu A, Porcu EP, Piras S, Ibba R, Carta A, Mollicotti P, et al. Solid lipid nanoparticles as formulative strategy to increase oral permeation of a molecule active in multidrug-resistant tuberculosis management. *Pharmaceutics*. 2020;12(12):1–24.
  59. Sun W, Zou W, Huang G, Li A, Zhang N. Pharmacokinetics and targeting property of TFu-loaded liposomes with different sizes after intravenous and oral administration. *J Drug Target*. 2008;16(5):357–65.
  60. Emami J, Mohiti H, Hamishehkar H, Varshosaz J. Formulation and optimization of solid lipid nanoparticle formulation for pulmonary delivery of budesonide using Taguchi and Box-Behnken design. *Res Pharm Sci*. 2015;10(1):17–33. Available from: <https://pubmed.ncbi.nlm.nih.gov/26430454>
  61. Attia IA, El-Gizawy SA, Fouda MA, Donia AM. Influence of a niosomal formulation on the oral bioavailability of acyclovir in rabbits. *AAPS PharmSciTech*. 2007;8(4):1–7.
  62. Chen Y, Chen J, Cheng Y, Luo L, Zheng P, Tong Y, et al. A lyophilized sterically stabilized liposome-containing docetaxel: in vitro and in vivo evaluation. *J Liposome Res*. 2017;27(1):64–73.
  63. Ertekin Z, Bayindir Z, Yuksel N. Stability studies on piroxicam encapsulated niosomes. *Curr Drug Deliv*. 2015;12(2):192–9.
  64. Vertzoni M, Augustijns P, Grimm M, Koziolok M, Lemmens G, Parrott N, et al. Impact of regional differences along the gastrointestinal tract of healthy adults on oral drug absorption: an UNGAP review. *Eur J Pharm Sci*. 2019;134(April):153–75.
  65. Shokri M, Tavallaie M, Hosseini SM. Effect of lyophilization on the size and polydispersity of unilamellar and multilamellar liposomes. *J Nanotechnol Mater Sci*. 2016;3(2):1–4.

**Publisher's Note** Springer Nature remains neutral with regard to jurisdictional claims in published maps and institutional affiliations.